

Rotatable Antenna-Enhanced Cell-Free Communication

Kecheng Pan, Beixiong Zheng, *Senior Member, IEEE*, Yanhua Tan, Emil Björnson, *Fellow, IEEE*, Robert Schober, *Fellow, IEEE*, and Rui Zhang, *Fellow, IEEE*

Abstract—Rotatable antenna (RA) is a promising technology that can exploit new spatial degrees-of-freedom (DoFs) by flexibly adjusting the three-dimensional (3D) boresight direction of antennas. In this letter, we investigate an RA-enhanced cell-free system for downlink transmission, where multiple RA-equipped access points (APs) cooperatively serve multiple single-antenna users over the same time-frequency resource. Specifically, we aim to maximize the sum rate of all users by jointly optimizing the AP-user associations and the RA boresight directions. Accordingly, we propose a two-stage strategy to solve the AP-user association problem, and then employ fractional programming (FP) and successive convex approximation (SCA) techniques to optimize the RA boresight directions. Numerical results demonstrate that the proposed RA-enhanced cell-free system significantly outperforms various benchmark schemes.

Index Terms—Rotatable antenna (RA), cell-free MIMO, antenna boresight optimization, user association, fractional programming.

I. INTRODUCTION

With the rapid development of global information and communication technology (ICT), the denser deployment of access points (APs) has become a prevailing trend in communication systems to meet the increasing demands for lower latency, higher reliability, and improved spectral efficiency. A promising paradigm is the cell-free multiple-input multiple-output (MIMO) system [1]. In this system, numerous APs, distributed throughout the service area and connected to a central processing unit (CPU) via fronthaul, collaboratively serve all users without cell boundaries [2]. However, conventional cell-free MIMO systems typically employ isotropic and fixed antennas, lacking the capability to dynamically distribute antenna resources in the spatial domain. This inherent limitation consequently restricts the communication performance.

To overcome this limitation, rotatable antenna (RA) [5]–[9] has recently emerged as a promising technology to exploit new spatial degrees-of-freedom (DoFs) by dynamically adjusting the antennas' three-dimensional (3D) boresight directions. As a simplified yet appealing variant of the six-dimensional movable antenna (6DMA) [3], [4] paradigm leveraging only the rotation flexibility (without changing antenna positions), RA enables a cost-effective and compact design more suitable for practical deployment [5]. Due to these appealing advantages, recent studies have explored the performance gains enabled by RA in various wireless systems. The authors in [6] and [7] established the fundamental system model and channel characteristics of RA systems, demonstrating their ability to achieve more favorable channel conditions. Building on this, RA has been applied to more challenging scenarios, such as integrated sensing and communication (ISAC) [8] and physical-layer security [9]. Notably, through flexible 3D boresight control,

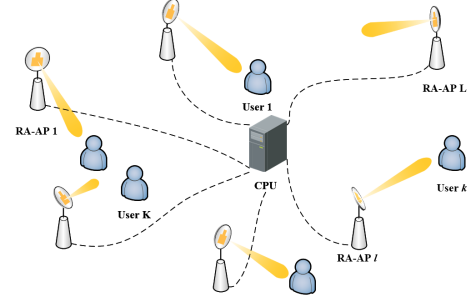


Fig. 1. Cell-free system with RA-equipped APs.

RA can enhance the signal in desired directions, thereby making it well-suited for improving the communication performance of cell-free systems. Nevertheless, the application of RA in such systems remains unexplored, thus motivating further investigation in this work.

Motivated by the above, in this letter, we investigate an RA-enhanced cell-free MIMO system for downlink transmission (as shown in Fig. 1), where multiple RA-equipped APs collaboratively provide communication services to distributed users. To enhance the communication quality of users, we formulate an optimization problem for maximizing their sum rate by jointly designing the AP-user associations and the RA boresight directions. As the formulated problem is non-convex, we propose a two-stage algorithm to determine the AP-user associations, and then apply fractional programming (FP) with successive convex approximation (SCA) to produce high-quality solutions for the RA boresight directions. Simulation results show that RA can enhance the sum rate of all users, significantly outperforming various benchmark schemes.

II. SYSTEM MODEL AND PROBLEM FORMULATION

As shown in Fig. 1, we consider an RA-enhanced downlink cell-free network consisting of L APs and K users, where $L \geq K$. Each AP is equipped with a directional RA, while each user employs a single isotropic antenna. All APs are connected to a CPU via a fronthaul network and cooperatively serve users over the same time-frequency resource. Let $\mathcal{L} = \{1, 2, \dots, L\}$ and $\mathcal{K} = \{1, 2, \dots, K\}$ denote the index sets of the APs and users, respectively. Without loss of generality, we assume that all APs and users are located in a global Cartesian coordinate system (CCS). Let $\mathbf{v}_l \in \mathbb{R}^{3 \times 1}$, $l \in \mathcal{L}$, and $\mathbf{q}_k \in \mathbb{R}^{3 \times 1}$, $k \in \mathcal{K}$ denote the positions of AP l and user k , respectively. Let $d_{l,k} = \|\mathbf{q}_k - \mathbf{v}_l\|$ denote the distance between AP l and user k , where $\|\cdot\|$ is the Euclidean norm.

A. Channel Model

In this letter, we assume a generic directional gain pattern for each RA as [6]

$$G_e(\epsilon, \varphi) = \begin{cases} G_0 \cos^{2p}(\epsilon), & \epsilon \in [0, \frac{\pi}{2}), \varphi \in [0, 2\pi) \\ 0, & \text{otherwise,} \end{cases} \quad (1)$$

where (ϵ, φ) is a pair of incident angles with respect to the RA boresight direction, p denotes the directivity factor, and $G_0 = 2(2p+1)$ denotes the maximum gain in the boresight direction. Let \mathbf{f}_l denote the RA pointing vector at AP l . Accordingly, the directional gain of the RA at AP l in the direction of user k can be expressed as $G_{l,k} = G_0 \cos^{2p}(\epsilon_{l,k})$, where $\cos(\epsilon_{l,k}) \triangleq$

Kecheng Pan, Beixiong Zheng, and Yanhua Tan are with the School of Microelectronics, South China University of Technology, Guangzhou 511442, China (e-mails: 202421065214@mail.scut.edu.cn; bxzheng@scut.edu.cn; tanyanhua06@163.com).

Emil Björnson is with the Division of Communication Systems, KTH Royal Institute of Technology, 100 44 Stockholm, Sweden (e-mail: emilbjo@kth.se).

Robert Schober is with the Institute for Digital Communications, Friedrich Alexander-University Erlangen-Nürnberg, 91054 Erlangen, Germany (e-mail: robert.schober@fau.de).

Rui Zhang is with the Department of Electrical and Computer Engineering, National University of Singapore, Singapore 117583 (e-mail: elezhang@nus.edu.sg).

$\vec{f}_l^T \vec{q}_{l,k}$ is the projection between \vec{f}_l^T and $\vec{q}_{l,k}$ with $\vec{q}_{l,k} \triangleq \frac{\mathbf{q}_k - \mathbf{v}_l}{d_{l,k}}$ denoting the normalized direction vector from AP l to user k .

We assume that the channel from AP l to user k experiences quasi-static flat-fading, which can be modeled as

$$h_{l,k}(\vec{f}_l) = \sqrt{\beta(d_{l,k}) G_{l,k} g_{l,k}}, \quad (2)$$

where $\beta(d_{l,k})$ denotes the large-scale channel power gain due to the distance-dependent path loss and shadowing, and $g_{l,k}$ models the small-scale channel fading. Specifically, $\beta(d_{l,k})$ is modeled as

$$\beta(d_{l,k}) = C_0 (d_0/d_{l,k})^\alpha, \quad (3)$$

where C_0 represents the channel power gain at the reference distance $d_0 = 1$ m, and α is the path loss exponent. Furthermore, we assume that $g_{l,k}$ follows an independent Rician fading distribution, characterized by Rician factor κ and given by

$$g_{l,k} = \sqrt{\frac{\kappa}{\kappa+1}} \bar{g}_{l,k} + \sqrt{\frac{1}{\kappa+1}} \tilde{g}_{l,k}, \quad (4)$$

where $\bar{g}_{l,k} = e^{-j\frac{2\pi}{\lambda} d_{l,k}}$ denotes the line-of-sight (LoS) component of the channel, and $\tilde{g}_{l,k} \sim \mathcal{CN}(0, 1)$ denotes the non-LoS (NLoS) channel component modeled by Rayleigh fading, with $\mathcal{CN}(0, 1)$ denoting a circularly symmetric complex Gaussian (CSCG) distribution with mean zero and unit covariance.

B. Signal Model

Since a single RA can only steer its antenna boresight toward one direction at a time, serving multiple users simultaneously would disperse the signal power. Therefore, for simplicity, we assume that each AP serves only one user at a time. Moreover, we use the matrix $\mathbf{B} \in \mathbb{R}^{L \times K}$ to represent the AP-user associations, which can be written as

$$\mathbf{B} = \begin{bmatrix} b_{1,1} & \cdots & b_{1,K} \\ \vdots & \ddots & \vdots \\ b_{L,1} & \cdots & b_{L,K} \end{bmatrix}, \quad (5)$$

where $b_{l,k} = \{0, 1\}, \forall l \in \mathcal{L}, \forall k \in \mathcal{K}$, is a binary indicator for the association between AP l and user k , where $b_{l,k} = 1$ indicates that user k is served by AP l ; otherwise $b_{l,k} = 0$.

As a prerequisite for precoding and subsequent optimization, we assume that the global channel state information (CSI) can be fully acquired by the CPU via the fronthaul [10], [11]. In addition, to achieve coherent superposition and maximize the received signal power, we adopt normalized conjugate beamforming with precoding factor $\phi_{l,k}^* \triangleq \frac{h_{l,k}^*}{|h_{l,k}|}$. Thus, the downlink transmitted signal s_l at AP l can be written as

$$s_l = \sqrt{P} \sum_{k=1}^K b_{l,k} \phi_{l,k}^* x_k, \quad (6)$$

where P denotes the transmit power of the AP, x_k represents the data signal intended for user k , with $\mathbb{E}\{|x_k|^2\} = 1$. Consequently, the received signal at user k can be expressed as

$$y_k(\vec{f}_l) = \underbrace{\sum_{l=1}^L h_{l,k}(\vec{f}_l) s_l}_{\text{Desired signal}} + n_k = \underbrace{\sqrt{P} \sum_{l=1}^L h_{l,k}(\vec{f}_l) b_{l,k} \phi_{l,k}^* x_k}_{\text{Desired signal}} + \underbrace{\sqrt{P} \sum_{i \neq k} \sum_{l=1}^L h_{l,i}(\vec{f}_l) b_{l,i} \phi_{l,i}^* x_i}_{\text{Inter-user interference}} + n_k, \quad (7)$$

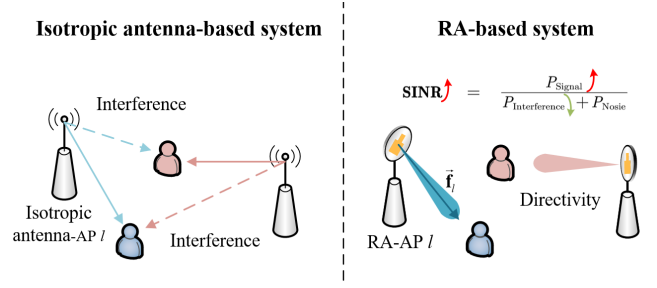


Fig. 2. Comparison between an isotropic antenna-based system and an RA-based system.

where $n_k \sim \mathcal{CN}(0, \sigma^2)$ represents complex additive white Gaussian noise (AWGN) with variance σ^2 . Thus, the received signal-to-interference-plus-noise ratio (SINR) at user k can be expressed as

$$\gamma_k = \frac{P \left| \sum_{l=1}^L h_{l,k}(\vec{f}_l) b_{l,k} \phi_{l,k}^* \right|^2}{P \left| \sum_{i \neq k} \sum_{l=1}^L h_{l,i}(\vec{f}_l) b_{l,i} \phi_{l,i}^* \right|^2 + \sigma^2}. \quad (8)$$

Accordingly, the achievable rate of user k can be expressed as

$$R_k = \log_2(1 + \gamma_k). \quad (9)$$

In this letter, we aim to jointly optimize the AP-user associations and the RA pointing vectors to maximize the sum rate of users. Accordingly, the optimization problem is formulated as

$$(P1) : \max_{\mathcal{F}, \mathbf{B}} \sum_{k=1}^K R_k \quad (10a)$$

$$\text{s.t. } \|\vec{f}_l\| = 1, \forall l, \quad (10b)$$

$$\sum_{l=1}^L b_{l,k} \geq 1, \forall k \in \mathcal{K}, \quad (10c)$$

$$\sum_{k=1}^K b_{l,k} = 1, \forall l \in \mathcal{L}, \quad (10d)$$

where $\mathcal{F} = \{\vec{f}_1, \dots, \vec{f}_L\}$ denotes the collection of RA pointing vectors. Constraint (10b) enforces the unit-norm condition for each pointing vector, (10c) ensures that each user is served by at least one AP for fairness, and (10d) ensures that each AP only provides services to one user. Note that (P1) is challenging to solve due to the non-concave objective (10a) and the non-convex constraint (10b). To efficiently address the problem, we first propose a two-stage strategy to obtain the AP-user association matrix, and then develop a fractional programming-based algorithm to optimize the RA pointing vectors.

Before solving (P1), we first illustrate the benefits of RA-based systems compared to conventional isotropic antenna-based systems in Fig. 2. In isotropic antenna-based systems, as the antennas' broadcast signals uniformly in all directions, severe inter-user interference may occur. In contrast, in RA-based systems, the 3D boresight direction of each antenna can be adaptively adjusted toward the intended user, strengthening the desired signal while reducing interference to other users, thereby improving the overall SINR of users.

III. PROPOSED ALGORITHM

In this section, to tackle the non-convexity of Problem (P1), which involves integer variables and intricate coupling between the association matrix \mathbf{B} and the RA pointing vectors \mathcal{F} , we decompose it into two sequential stages. We first

develop a two-stage AP–user association strategy to obtain the association matrix \mathbf{B} . Subsequently, we propose a fractional programming-based algorithm to optimize the RA pointing vector at each AP, aiming to maximize the system sum rate.

A. AP-User Association Strategy

By exploiting the fact that nearer AP–user pairs suffer less attenuation and are more likely to achieve better performance, we form an approximate substitution to (P1). Specifically, by calculating the distances $d_{l,k}$ of all possible AP–user pairs, we can reformulate the original association problem as minimizing the total AP–user association distance $D_{\text{sum}} = \sum_{l=1}^L \sum_{k=1}^K b_{l,k} d_{l,k}$. Accordingly, we have:

$$(P2) : \min_{b_{l,k}} D_{\text{sum}} \quad (11a)$$

$$\text{s.t. } b_{l,k} \in \{0, 1\}, \forall l \in \mathcal{L}, \forall k \in \mathcal{K}, \quad (11b)$$

$$\sum_{l=1}^L b_{l,k} \geq 1, \forall k \in \mathcal{K}, \quad (11c)$$

$$\sum_{k=1}^K b_{l,k} = 1, \forall l \in \mathcal{L}. \quad (11d)$$

Note that constraint (11b) defines the problem as a zero-one optimization problem, (11c) ensures that each user is associated with at least one AP, and (11d) ensures that each AP serves only one user. To address this non-convex problem, we propose a two-stage AP–user association strategy based on the AP–user distances. As summarized in Algorithm 1, the proposed strategy consists of two stages:

1) *Initial AP-User Association*: At this stage, we aim to allocate each user to a unique AP for fairness, while ensuring that the distance of each paired AP–user is as small as possible. To begin with, we initialize the index sets of unpaired APs and users as $\mathcal{L}^{(0)} = \mathcal{L}$ and $\mathcal{K}^{(0)} = \mathcal{K}$ with $|\mathcal{L}^{(0)}| = L$ and $|\mathcal{K}^{(0)}| = K$, and set the AP–user association matrix to $\mathbf{B} = \mathbf{0}_{L \times K}$, with $\mathbf{0}_{L \times K}$ denoting the $L \times K$ all-zero matrix. Next, we calculate the distances $\{d_{l,k}\}_{l \in \mathcal{L}, k \in \mathcal{K}}$ between all possible AP–user pairs. Based on these distances, we iteratively allocate K out of L APs to the K users until each user is associated with a unique AP. Specifically, in the j -th iteration, let $\mathcal{L}^{(j-1)}$ and $\mathcal{K}^{(j-1)}$ denote the sets of unpaired AP and user indexes obtained from the $(j-1)$ -th iteration, where we have $|\mathcal{L}^{(j-1)}| = L - (j-1)$ and $|\mathcal{K}^{(j-1)}| = K - (j-1)$. Then, we select the AP–user pair $(l^{(j)}, k^{(j)})$ that corresponds to the minimum $d_{l,k}$ among the unpaired AP and user sets:

$$(l^{(j)}, k^{(j)}) = \arg \min_{l \in \mathcal{L}^{(j-1)}, k \in \mathcal{K}^{(j-1)}} d_{l,k}. \quad (12)$$

According to (12), AP $l^{(j)}$ is allocated to user $k^{(j)}$. This allocation is recorded in matrix \mathbf{B} as

$$b_{l^{(j)}, k^{(j)}} = 1 \Rightarrow \mathbf{B} \left(l^{(j)}, k^{(j)} \right) = 1. \quad (13)$$

Thereafter, we remove the indexes of AP $l^{(j)}$ and user $k^{(j)}$ from $\mathcal{L}^{(j-1)}$ and $\mathcal{K}^{(j-1)}$, respectively, yielding

$$\mathcal{L}^{(j)} = \mathcal{L}^{(j-1)} \setminus \{l^{(j)}\}, \quad (14a)$$

$$\mathcal{K}^{(j)} = \mathcal{K}^{(j-1)} \setminus \{k^{(j)}\}. \quad (14b)$$

Upon completion of K iterations, the set of unpaired users becomes empty ($\mathcal{K}^{(K)} = \emptyset$), confirming that each user is served by exactly one AP in compliance with constraint (11c).

2) *Remaining AP Assignment*: Since larger AP–user distances yield weaker links and offer limited gains for sum-rate maximization, it is preferable to associate users with nearby APs. Therefore, at this stage, we aim to assign each of the remaining $|\mathcal{L}^{(K)}| = L - K$ unpaired APs to its nearest user.

Algorithm 1 Two-stage AP–user association strategy.

Input L, K , AP and user positions.

Initialization $\mathcal{L}^{(0)} = \mathcal{L}$, $\mathcal{K}^{(0)} = \mathcal{K}$, $\mathbf{B} = \mathbf{0}_{L \times K}$.

Stage 1:

1: Calculate $d_{l,k}, \forall l \in \mathcal{L}, \forall k \in \mathcal{K}$.

2: **for** $j = 1$ to K **do**

3: For $l \in \mathcal{L}^{(j-1)}, k \in \mathcal{K}^{(j-1)}$, find the minimum $d_{l,k}$ and the corresponding AP–user pair $(l^{(j)}, k^{(j)})$.

4: Allocate AP $l^{(j)}$ to user $k^{(j)}$, and update \mathbf{B} .

5: Remove $l^{(j)}$ from $\mathcal{L}^{(j-1)}$ and $k^{(j)}$ from $\mathcal{K}^{(j-1)}$.

6: **end for**

Stage 2:

7: **for** each AP $l \in \mathcal{L}^{(K)}$ **do**

8: Find the nearest user $k^{[l]}$.

9: Allocate AP l to user $k^{[l]}$, and update \mathbf{B} .

10: **end for**

Output AP–user association matrix \mathbf{B} .

For each unpaired AP, denoted by $l \in \mathcal{L}^{(K)}$, we find the user $k^{[l]}$ that is closest to AP l , i.e.,

$$k^{[l]} = \arg \min_{k^{[l]} \in \mathcal{K}} d_{l,k}, \quad l \in \mathcal{L}^{(K)}. \quad (15)$$

AP l is then allocated to user $k^{[l]}$, and the allocation is recorded in \mathbf{B} . The final output is the AP–user association matrix \mathbf{B} , representing the overall AP–user associations.

The proposed algorithm ensures that each user is served by at least one AP and that no AP remains idle. It should be noted that (P2) is an approximate surrogate of (P1), obtained by omitting the effect of small-scale fading. Although this leads to suboptimal solutions, Algorithm 1 provides an effective AP–user association with low computational complexity, requiring only basic operations such as sorting and comparison. Specifically, the complexity order for solving problem (P2) is $\mathcal{O}(KL)$.

B. RA Pointing Vector Optimization

After AP–user association, our objective is to optimize the RA pointing vectors at the APs. Accordingly, we simplify problem (P1) as follows:

$$(P3) : \max_{\mathcal{F}} \sum_{k=1}^K R_k \quad (16a)$$

$$\text{s.t. } \|\vec{\mathbf{f}}_l\| = 1, \forall l. \quad (16b)$$

As the achievable rate R_k in (16a) contains complex fractional structures, problem (P3) is challenging to solve directly. Therefore, we apply the quadratic transform to the SINR term in R_k , yielding the following equivalent problem:

$$(P4) : \max_{\mathcal{F}, \mathcal{Z}} \sum_{k=1}^K \log_2 \left(1 + \tilde{\gamma}_k \left(\vec{\mathbf{f}}_l, z_k \right) \right) \quad (17a)$$

$$\text{s.t. } \|\vec{\mathbf{f}}_l\| = 1, \forall l, \quad (17b)$$

where z_k is introduced by the quadratic transform for each user k , and $\mathcal{Z} = \{z_1, \dots, z_K\}$ denotes the collection of z_k . The quadratic transform reformulates the SINR γ_k in the objective function as

$$\tilde{\gamma}_k \left(\vec{\mathbf{f}}_l, z_k \right) = 2\sqrt{P} \operatorname{Re} \left\{ z_k \left(\sum_{l=1}^L h_{l,k} \left(\vec{\mathbf{f}}_l \right) b_{l,k} \phi_{l,k}^* \right) \right\} - |z_k|^2 \left(P \left| \sum_{i \neq k} \sum_{l=1}^L h_{l,k} \left(\vec{\mathbf{f}}_l \right) b_{l,i} \phi_{l,i}^* \right|^2 + \sigma^2 \right), \quad (18)$$

where $\text{Re}\{\cdot\}$ denotes the real part of a complex number. Subsequently, we alternately optimize $\vec{\mathbf{f}}_l$ and z_k to maximize the objective function (17a). For given $\vec{\mathbf{f}}_l$, the optimal z_k has the following closed-form solution [12]:

$$z_k^* = \frac{\sum_{l=1}^L \sqrt{P} h_{l,k}(\vec{\mathbf{f}}_l) b_{l,k} \phi_{l,k}^*}{P \left| \sum_{i \neq k} \sum_{l=1}^L h_{l,k}(\vec{\mathbf{f}}_l) b_{l,i} \phi_{l,i}^* \right|^2 + \sigma^2}. \quad (19)$$

Next, we focus on optimizing $\vec{\mathbf{f}}_l$ for given z_k . As $G_{l,k}(\vec{\mathbf{f}}_l)$ in $h_{l,k}$ is a piecewise function, objective function (17a) remains non-convex. To address this issue, we approximate $G_{l,k}(\vec{\mathbf{f}}_l)$ using the softplus function, which provides a smooth and differentiable surrogate as

$$G'_{l,k}(\vec{\mathbf{f}}_l) = G_0 \left[\frac{\ln(1 + e^{m \vec{\mathbf{f}}_l^T \bar{\mathbf{q}}_{l,k}})}{m} \right]^{2p}, \quad (20)$$

where m controls the smoothness of the approximation. In addition, we apply successive convex approximation (SCA), iteratively approximating (17a) with a convex surrogate. Without loss of generality, we present the process of the $(i+1)$ -th iteration, where the values of $\vec{\mathbf{f}}_l$ obtained in the i -th iteration are denoted by $\vec{\mathbf{f}}_l^{(i)}$. By using the first-order Taylor expansion at $\vec{\mathbf{f}}_l$, $h_{l,k}(\vec{\mathbf{f}}_l)$ can be linearized as $\Lambda_{l,k}^{(i+1)}$, and objective (17a) can be established as $U(\vec{\mathbf{f}}_l)$, both of which are shown at the bottom of this page.

Thus, problem (P4) can be transformed to

$$(P5) : \max_{\mathcal{F}} U(\vec{\mathbf{f}}_l) \quad (23a)$$

$$\text{s.t. (16b)}. \quad (23b)$$

However, problem (P5) remains non-convex due to the unit-norm constraint on $\vec{\mathbf{f}}_l$. To address this, we relax the equality constraint (16b) as $\|\vec{\mathbf{f}}_l\| \leq 1$, yielding the following problem,

$$(P6) : \max_{\mathcal{F}} U(\vec{\mathbf{f}}_l) \quad (24a)$$

$$\text{s.t. } \|\vec{\mathbf{f}}_l\| \leq 1, \forall l. \quad (24b)$$

It can be verified that problem (P6) is convex and can be solved by the CVX solver [13]. Note that the optimal value obtained by problem (P6) serves as an upper bound for that of problem (P5) due to the relaxation of the equality constraint (16b). After obtaining the optimal solutions of $\vec{\mathbf{f}}_l$ through Algorithm 2, the pointing vector needs to be recovered as a unit vector, i.e., $\vec{\mathbf{f}}_l^* = \frac{\vec{\mathbf{f}}_l}{\|\vec{\mathbf{f}}_l\|}$. This normalization only scales $\vec{\mathbf{f}}_l$ to unit length without altering its direction.

We summarize the proposed fractional programming-based algorithm in Algorithm 2. Since the optimal objective function is non-decreasing over the iterations, Algorithm 2 is guaranteed to converge. In terms of computational complexity, the cost of updating z_k is negligible, while optimizing $\vec{\mathbf{f}}_l$ in (P6) incurs a complexity of $\mathcal{O}(L^{3.5} \ln(1/\varepsilon))$ per iteration, where ε denotes the accuracy threshold for convergence. Hence, the overall complexity of Algorithm 2 is $\mathcal{O}(IL^{3.5} \ln(1/\varepsilon))$, where I represents the number of iterations required for convergence.

Algorithm 2 Fractional Programming-based Algorithm.

Input: Pointing vector $\vec{\mathbf{f}}_l^{(0)}$ and threshold $\xi > 0$.

Initialization: $i \leftarrow 0$.

repeat

 Given $\vec{\mathbf{f}}_l^{(i)}$, calculate $z_k^{(i+1)}$ according to (19).

 Given $z_k^{(i+1)}$ and $\vec{\mathbf{f}}_l^{(i)}$, obtain $\vec{\mathbf{f}}_l^{(i+1)}$ by solving problem (P6).

 Update $i = i + 1$.

until The fractional increase of the sum rate in (17a) falls below the threshold ξ or the iteration number i reaches the pre-designed number of iterations I .

Output: $\vec{\mathbf{f}}_l = \vec{\mathbf{f}}_l^{(i)}$ and $z_k = z_k^{(i)}$.

IV. SIMULATION RESULTS

In this section, we evaluate an RA-enhanced downlink cell-free system employing the proposed AP-user association strategy and fractional programming-based algorithm. We consider L APs and K users randomly distributed in a 300 m \times 300 m area, where each AP employs an RA with directivity factor $p = 2$. The system operates at 2.4 GHz ($\lambda = 0.125$ m) with noise power $\sigma^2 = -80$ dBm. Unless otherwise stated, parameters are set as $P = 20$ dBm, $\beta_0 = -30$ dB, $\alpha = 2$, $\kappa = 1$, and $m = 20$ (as in [14]). In the following, results are averaged over 100 random Monte Carlo realizations, and the proposed algorithm for RA pointing vector optimization is compared with the following benchmark schemes:

- **Fixed directional antenna-based scheme:** In this scheme, the pointing vectors are fixed as $\vec{\mathbf{f}}_l = [1, 0, 0]^T, \forall l$.
- **Isotropic antenna-based scheme:** In this scheme, the directional gain in (1) is replaced by $G_e(\epsilon, \varphi) = G_0 \cos^{2p}(\epsilon)$, with $G_0 = 1$ and $p = 0$.
- **RA-user alignment scheme:** In this scheme, each RA steers its boresight directly toward its associated user.

In Fig. 3, we illustrate the convergence behavior of the proposed algorithms. As expected, for all considered numbers of APs L , the sum rate increases monotonically with the number of iterations. Although an increased number of APs results in marginally slower convergence, all configurations converge within 10 iterations, verifying the algorithm's effectiveness.

Fig. 4 illustrates the sum rate performance versus the number of APs L for a fixed number of users $K = 5$. As expected, the sum rate increases with L for all considered schemes. Moreover, the proposed RA-based scheme and the RA-user alignment scheme consistently outperform all other benchmark schemes. This performance gain is mainly due to the capability of RAs to dynamically steer their boresight directions toward the desired users, thereby focusing the radiation power for SINR enhancement. Notably, the proposed RA-based scheme achieves an additional performance gain over the RA-user alignment baseline. This underscores the effectiveness of the proposed joint optimization algorithm, which also accounts for the impact of inter-user interference rather than merely pursuing the maximization of the associated user's signal power.

$$\Lambda_{l,k}^{(i+1)}(\vec{\mathbf{f}}_l) \triangleq h_{l,k}(\vec{\mathbf{f}}_l^{(i)}) + p \sqrt{\beta(d_{l,k}) G_0 g_{l,k}} \left(\frac{\ln(1 + e^{m \vec{\mathbf{f}}_l^{(i)T} \bar{\mathbf{q}}_{l,k}})}{m} \right)^{p-1} \frac{e^{m \vec{\mathbf{f}}_l^{(i)T} \bar{\mathbf{q}}_{l,k}}}{1 + e^{m \vec{\mathbf{f}}_l^{(i)T} \bar{\mathbf{q}}_{l,k}}} (\vec{\mathbf{f}}_l - \vec{\mathbf{f}}_l^{(i)})^T \bar{\mathbf{q}}_{l,k}. \quad (21)$$

$$U(\vec{\mathbf{f}}_l) \triangleq \sum_{k=1}^K \log_2 \left(1 + 2\sqrt{P} \text{Re} \left\{ z_k \left(\sum_{l=1}^L \Lambda_{l,k}^{(i+1)}(\vec{\mathbf{f}}_l) b_{l,k} \phi_{l,k}^* \right) \right\} - |z_k|^2 \left(P \left| \sum_{i \neq k} \sum_{l=1}^L \Lambda_{l,k}^{(i+1)}(\vec{\mathbf{f}}_l) b_{l,i} \phi_{l,i}^* \right|^2 + \sigma^2 \right) \right). \quad (22)$$

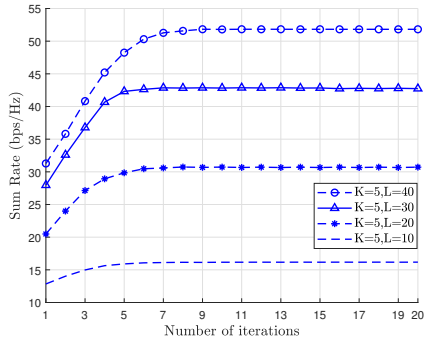


Fig. 3. Convergence behavior of the proposed algorithm.

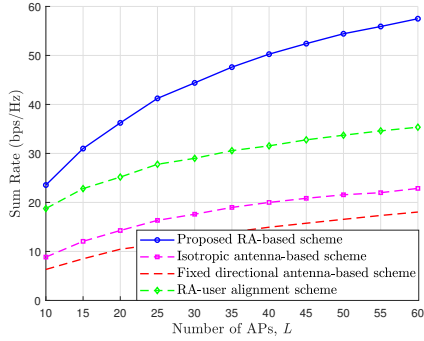


Fig. 4. Sum rate (bps/Hz) vs. the number of APs where $K = 5$.

Fig. 5 illustrates the average per-user rate versus the number of users K for different schemes. As K increases, the average per-user rate decreases for all considered schemes since more users will lead to more severe multiuser interference. Notably, the proposed RA-based scheme consistently achieves the best performance and demonstrates superior robustness against inter-user interference. This improvement is primarily attributed to the ability of RAs to adaptively rotate their boresight directions, thereby concentrating signal power toward intended users and reducing the interference caused by signal energy leakage to other users. In contrast, the fixed directional antenna-based scheme performs even worse than the isotropic antenna-based scheme, as its inability to adjust boresight directions leads to limited coverage and poor interference management. This observation highlights the importance of directional flexibility in enhancing overall communication quality.

Fig. 6 shows the cumulative distribution function (CDF) of the rate per user for the considered schemes. As compared to the RA-user alignment scheme, for the proposed RA-based scheme, a greater proportion of users achieve high data rates, indicating that optimized boresight control significantly improves per-user performance. In addition, the fixed directional antenna-based scheme results in zero-rate transmission for a subset of users, primarily due to its inability to adapt the boresight directions, which leads to coverage blind spots.

V. CONCLUSION

In this letter, we proposed a novel RA-enhanced cell-free system, where the RA pointing vectors can be adjusted to change the directional gain pattern for maximizing the system sum rate. Specifically, we developed a two-stage strategy to solve the AP-user association problem and a fractional programming-based algorithm to obtain a high-quality solution for the RA pointing vectors. Simulation results demonstrate that, by optimizing each RA's pointing vector, the RA-equipped APs significantly enhance the directional gain toward

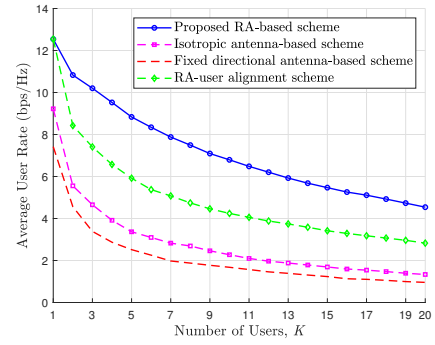


Fig. 5. Average per-user rate (bps/Hz) vs. the number of users where $L = 30$.

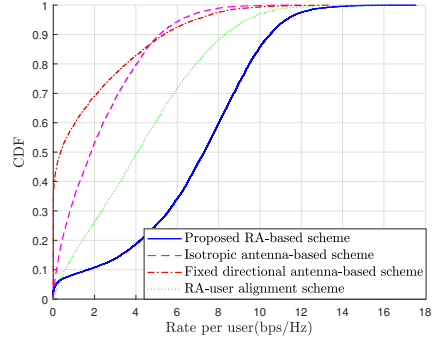


Fig. 6. CDF of rate per user, where $K = 10$ and $L = 30$.

intended users while suppressing interference in undesired directions, thereby achieving a higher system sum rate than various benchmark schemes.

REFERENCES

- [1] W. Jiang, B. Han, M. A. Habibi, and H. D. Schotten, "The road towards 6G: A comprehensive survey," *IEEE Open J. Commun. Soc.*, vol. 2, pp. 334–366, Feb. 2021.
- [2] Ö. Özdoğan, E. Björnson and J. Zhang, "Performance of cell-free massive MIMO with Rician fading and phase shifts," *IEEE Trans. Wireless Commun.*, vol. 18, no. 11, pp. 5299–5315, Nov. 2019.
- [3] X. Shao, Q. Jiang, and R. Zhang, "6D movable antenna based on user distribution: Modeling and optimization," *IEEE Trans. Wireless Commun.*, vol. 24, no. 1, pp. 355–370, Jan. 2025.
- [4] X. Shi, X. Shao, B. Zheng, and R. Zhang, "6DMA-aided cell-free massive MIMO communication," *IEEE Wireless Commun. Lett.*, vol. 14, no. 5, pp. 1361–1365, May 2025.
- [5] B. Zheng, T. Ma, C. You, J. Tang, R. Schober, and R. Zhang, "Rotatable antenna enabled wireless communication and sensing: Opportunities and challenges," *IEEE Wireless Commun.*, Early Access, 2025.
- [6] Q. Wu, B. Zheng, T. Ma, and R. Zhang, "Modeling and optimization for rotatable antenna enabled wireless communication," in *Proc. IEEE Int. Conf. Commun. (ICC)*, Montreal, Canada, Jun. 2025, pp. 1–6.
- [7] B. Zheng, Q. Wu, T. Ma, and R. Zhang, "Rotatable antenna enabled wireless communication: Modeling and optimization," *arXiv preprint arXiv:2501.02595*, 2025.
- [8] C. Zhou, C. You, B. Zheng, X. Shao and R. Zhang, "Rotatable antennas for integrated sensing and communications," *IEEE Wireless Commun. Lett.*, vol. 14, no. 9, pp. 2838–2842, Sept. 2025.
- [9] L. Dai, B. Zheng, Q. Wu, C. You, R. Schober, and R. Zhang, "Rotatable antenna-enabled secure wireless communication," *IEEE Wireless Commun. Lett.*, vol. 14, no. 11, pp. 3440–3444, Nov. 2025.
- [10] X. Xiong, B. Zheng, W. Wu, X. Shao, L. Dai, M. Zhao, and J. Tang, "Efficient channel estimation for rotatable antenna-enabled wireless communication," *IEEE Wireless Commun. Lett.*, vol. 14, no. 11, pp. 3719–3723, Nov. 2025.
- [11] E. Björnson and L. Sanguinetti, "Scalable cell-free massive MIMO systems," *IEEE Trans. Commun.*, vol. 68, no. 7, pp. 4247–4261, Jul. 2020.
- [12] K. Shen and W. Yu, "Fractional programming for communication systems—part I: power control and beamforming," *IEEE Trans. Signal Process.*, vol. 66, no. 10, pp. 2616–2630, May 2018.
- [13] S. Boyd and L. Vandenberghe, *Convex Optimization*. Cambridge, U.K.: Cambridge Univ. Press, Mar. 2004.
- [14] H. Q. Ngo, A. Ashikhmin, H. Yang, E. G. Larsson, and T. L. Marzetta, "Cell-free massive MIMO versus small cells," *IEEE Trans. Wireless Commun.*, vol. 16, no. 3, pp. 1834–1850, Mar. 2017.